Proceedings of the ASME 2014 33rd International Conference on Ocean, Offshore and Arctic Engineering
OMAE2014
June 8-13, 2014, San Francisco, California, USA

OMAE2014-24418

SEMI-SUBMERSIBLE HUB PLATFORM WITH AN INTERNAL DOCK MODEL TESTING

Edgard Borges Malta
TPN - Numerical Offshore Tank
Department of Naval Architecture
and Ocean Engineering
University of Sao Paulo
Sao Paulo, Brazil
edgard@tpn.usp.br

Felipe Ruggeri
TPN - Numerical Offshore Tank
Department of Naval Architecture
and Ocean Engineering
University of Sao Paulo
Sao Paulo, Brazil
felipe.ruggeri@tpn.usp.br

Pedro Cardozo de Mello
TPN - Numerical Offshore Tank
Department of Naval Architecture
and Ocean Engineering
University of Sao Paulo
Sao Paulo, Brazil
pedro.mello@tpn.usp.br

Eduardo M. Vilameá
E&P Department
PETROBRAS
Rio de Janeiro, Brazil
eduardo.vilamea@petrobras.com.br

Allan C. de Oliveira
R&D Department
PETROBRAS
Rio de Janeiro, Brazil
allan_carre@petrobras.com.br

Kazuo Nishimoto
TPN - Numerical Offshore Tank
Department of Naval Architecture
and Ocean Engineering
University of Sao Paulo
Sao Paulo, Brazil
kazuo@tpn.usp.br

ABSTRACT

The recent discoveries and development of the Pre-salt reservoir in Brazilian coast require a new logistical model for crew transportation and transhipment to the drilling and oil rigs due to the large distance from coast, harsh environment conditions and large amount of workers to be transported against the actual model adopted considering only transportation by helicopters in order to reduce overall costs. The adoption of a logistic model with maritime transportation in these scenarios could provide several advantages, however there are several challenges from the technical point of view in transhipment between ship-shaped vessels, that could represent a great limitation in terms of operational window. Previous works showed the feasibility of monocolumn platforms with an internal moonpool as a Logistic HUB [1], allowing the boat docking in sheltered conditions. This work shows an overview of the model testing of a semi-submersible with an internal dock and the comparison of the free-surface elevation and RAOs (Response Amplitude Operators) between experimental results and potential flow computations. The tests were performed for 5 headings considering 10 regular, 5 irregular and 1 transient waves under a single draft and 5 different devices to reduce wave energy in the interior region.

INTRODUCTION

The semi-submersible platform concept was developed as possible solution for deepwater offshore scenarios far from the coast under harsh environmental conditions. This platform can be applied as an offshore passenger hub in order to attend the huge passengers transport demand to production and drilling platforms in pre-sal reservoir in Brazilian coast. The transportation to offshore platforms has been performed by helicopter, which will be a very expensive solution for the high demand of passengers predicted in the next years, motivating

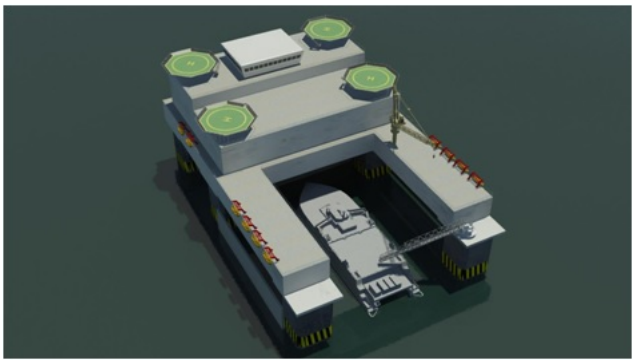

FIGURE 1. Illustrative concept of a passenger hub platform with internal dock.

alternative solutions. One competitive solution might be the transportation HSV (High Speed Vessels) between the coast to an offshore hub, where the workers are distributed to the platforms close to the hub by helicopters. The HSV transportation, on the other hand, presents a serious challenge during the people transfer from the boat to the unit due to the significant motions of the boat, which can lead to seasickness. One possible solution to mitigate this problem is to perform the operation in a sheltered area. The use of a semi-submersible platform can provide this sheltered area at its inner region if the adjacent columns are connected by some devices, such as a plate, in order to reduce wave energy inside as shown, for example, in the Fig. 1.

These sheltered areas can be achieved by using devices, such as flat panels, porous screens and/or vertical cavities in order diffract and break the waves, the first alternative "redirecting" the wave energy outside the dock (internal region) and the second one by dissipating the energy. The wave energy absorption by porous screens has been studied several times and the technique can be improved using two or more consecutive screens to provide vertical cavities and achieve a wave trapping effect. In [2] cavities between screens were employed to prevent wave reflection in front of a wave generator to avoid reflection during wave generation. The study suggests that a cavity between screens of 25% wavelength minimizes the reflection of waves through the screens. Similar results to a cavity of 15% of the wavelength were observed [3, 4]. [5] suggestes that a cavity of 25% wavelength width in a semi-submerged has reduced wave reflections. Several studies considering similar arrangements [6–8] provided the same conclusion, revealing the effectiveness of this technique to absorb waves. This absorption occurs by viscous dissipation and the effect can be amplified in the range between 15% and 25% wavelength of the incident wave due to cavity resonance, therefore this device was evaluated in the model tests although there is a lack of similarity concerning viscous effects.

It is well known that semi-submersible plaforms have small motions partially due to the reduced waterplane area, which provides high natural periods. The excitation forces are also small because most of the unit volume is concentrated in the keel and the wave pressure descreases exponentially with depth. The introduction of flat walls connecting adjacent columns to provide an internal dock can provide significant changes in the inner water behavior, related to the floating unit motions and diffraction pattern inside the dock.

In order to assess the ability to receive a vessel in the inner sheltered region and transfer passengers safely, a technical specification was defined by Petrobras and the TPN (Numerical Offshore Tank) to guarantee the operation feasibility. Based on this specification two types of structures were tested experimentally: monocolumn [1] and semi-submersible under a reduced scale of 1:80.

The main goal of the model test campaign was to evaluate the dock free surface elevation considering several absorbing devices and validate potential flow predictions, since the major goal of the project is to apply numerical computations to optimize the hub dimensions. Six absorbing devices configurations were proposed, as shown in Fig. 2:

1. Original configuration (OR), containing a horizontal constrain (flat plate) in the moonpool (inner) region, since its importance to reduce the free surface elevation was verified previously in the monocolumn tests;
2. Full side plates (PL), where vertical plates were installed between the adjacent columns from bottom to top but in the stern columns since it is the vessel entrance;
3. Middle side plates (MP), similar to the full side configuration, but the plates connect half the draft until the column top;
4. Installation of spreaders (diffration devices) in the side plates (ES) to produce wave scattering;
5. Installation of a collection of plates with vertical fringes (FR), also to produce diffraction and viscous dissipation in the openings;
6. Installation of a plastic mesh (TL) in between the vertical fringes to increase viscous effects.

The details concerning the several moonpool configuration can be seen in Fig. 3. The motions and free surface elevation were measured for 1 transient, 10 regular and 5 irregular (Jonswap spectra) waves, the latter equivalent to 3 hours in full scale model, considering a single load condition and 5 headings. The wave specifications can be seen in Table 1.

MODEL TEST DETAILS

The model was built in fiberglass under a 1:80 scale. The model scale was defined to guarantee that energy spectra was in the range between 0.5 and 1.5 Hz (Fig. 4), the basin limits

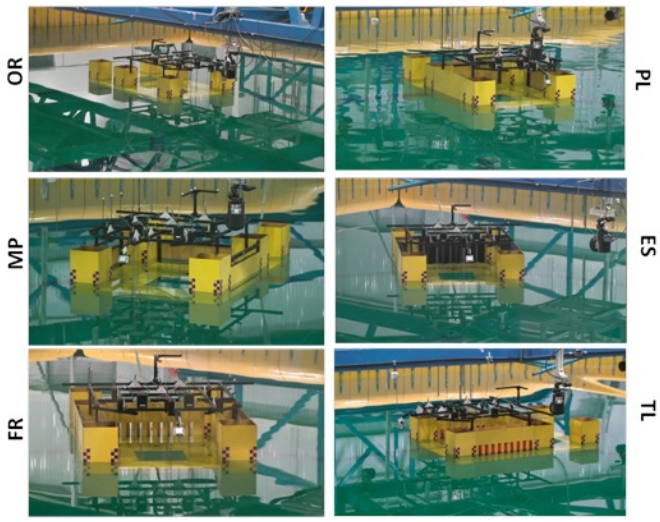

FIGURE 2. Overview of each conditions.

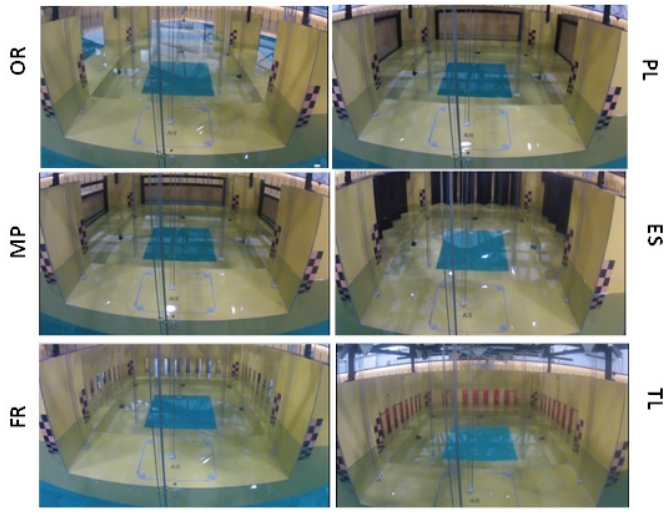

FIGURE 3. Moonpool detail for each condition.

for simultaneous wave generation and absorption. More details concerning the basin can be seen in [9]. The main dimensions and load condition are shown in Table 2. The ballast positioning and model calibration concerning mass, inertia and center of gravity position was performed using a three-dimensional model considering all devices (mainly wave-probes) installed, as can be seen in Fig. 5. The blue blocks represents the ballast used in the callibration and the comparison among the specified, expected from 3D computational model and measured properties are shown in Table 3.

The body motions in 6 DoF and free surface elevation were measured, the latter using 11 wave-probes installed in the dock,

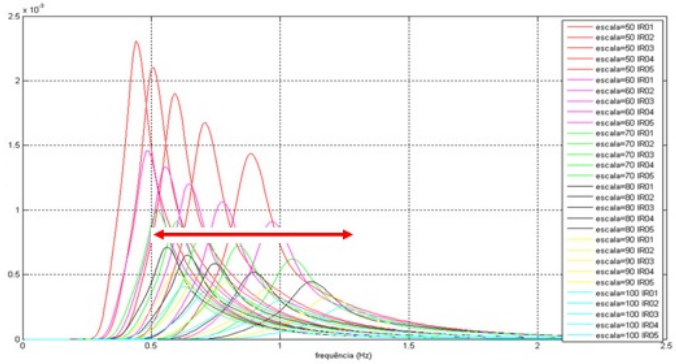

FIGURE 4. Effect of model scale in the frequency band of wave spectra.

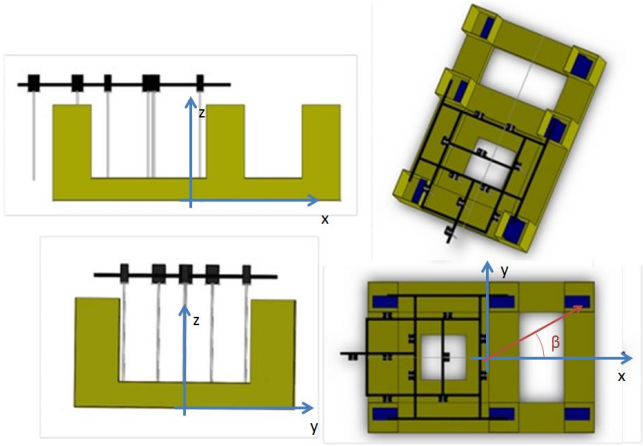

FIGURE 5. 3D numerical model constructed to estimate center of gravity and inertia. β indicates the incident wave direction.

as shown in details in Fig. 6 and [**?**]. The signals were cut to neglect transient effects and analyzed without any filter for both regular, irregular and transient waves. Spectral analysis were performed to obtain both Response Amplitude Operators (RAOs) were treated for each measured quantities during the tests. The results are presented considering the 6 DoF RAOs concerning the body motions and the 11 relative free surface elevation for the absorption devices that provided the highest efficiencies for 0 and 180^o headings, that were chosen since the behavior is quite different.

NUMERICAL MODEL

The main goal of the test was to validate the potential flow predictions concerning both body motions and relative free

TABLE 1. Wave specification - Full scale

Index	Tp (s)	Hs(m)
Irregular 1	8	4.5
Irregular 2	10	4.5
Irregular 3	12	4.5
Irregular 4	14	4.5
Irregular 5	16	4.5
Regular 1	8	4.5
Regular 2	9	4.5
Regular 3	10	4.5
Regular 4	11	4.5
Regular 5	12	4.5
Regular 6	13	4.5
Regular 7	14	4.5
Regular 8	15	4.5
Regular 9	16	4.5
Regular 10	17	4.5

TABLE 2. MODEL DIMENSIONS

	Prototype	Model	Unit
Length	150.0	1.875	m
Beam	100.0	1.25	m
Draft	30.0	0.375	m
Displacement	162360	0.317	ton
LCG	2.73	0.034	m
VCG	15.38	0.192	m
Rxx	37.69	0.471	m
Ryy	52.64	0.658	m

Orign is at the keel in the middle of the model.

surface elevation in the dock. Therefore a numerical computation was performed in *WAMIT*® [10]. The numerical model was set up considering high-order panels of 5 meters characteristic dimension and dock walls were modelled using dipole panels (Fig. [**?**]). The viscous effects concerning wave diffraction in the free surface elevation were completely neglected, considering

TABLE 3. Model verification

	$Mass(kg)$	$VCG(m)$	$I_{xx}(kg.m^2)$	$I_{yy}(kg.m^2)$	$I_{zz}(kg.m^2)$
Specified	309.4	0.192	68.7	133.9	180.6
Expected	308.8	0.188	68.3	135.9	190.0
Measured	308.8	0.197	69.2	127.9	
Diff.	−0.2%	2.5%	0.7%	1.5%	5.2%

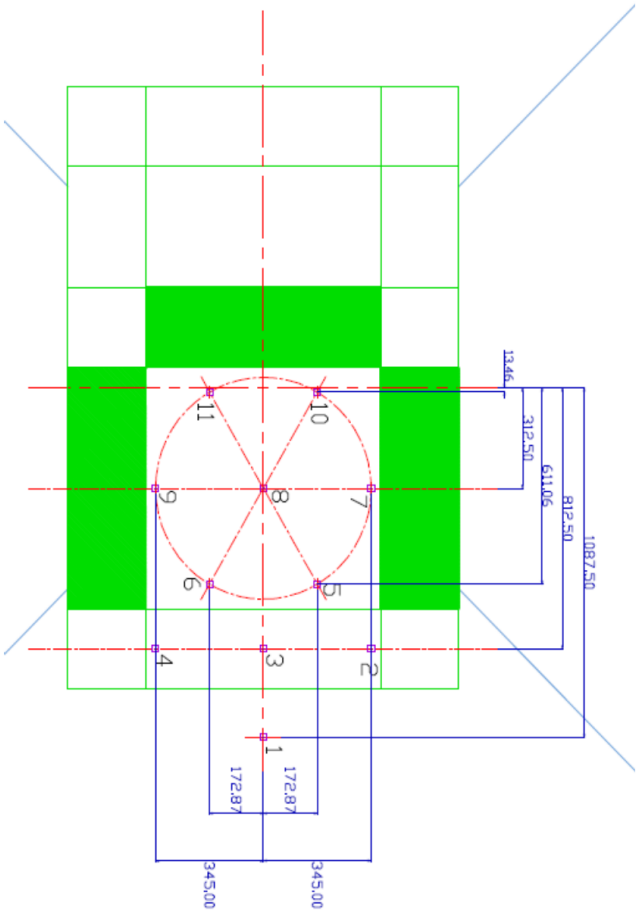

FIGURE 6. Arrangement of wave probes.

only external damping in the 6DoF *WAMIT*® to adjust the body motions.

RESULTS

The results concerning boy motions can be seen from Fig.9 to Fig.14 comparing both experimental results and numerical

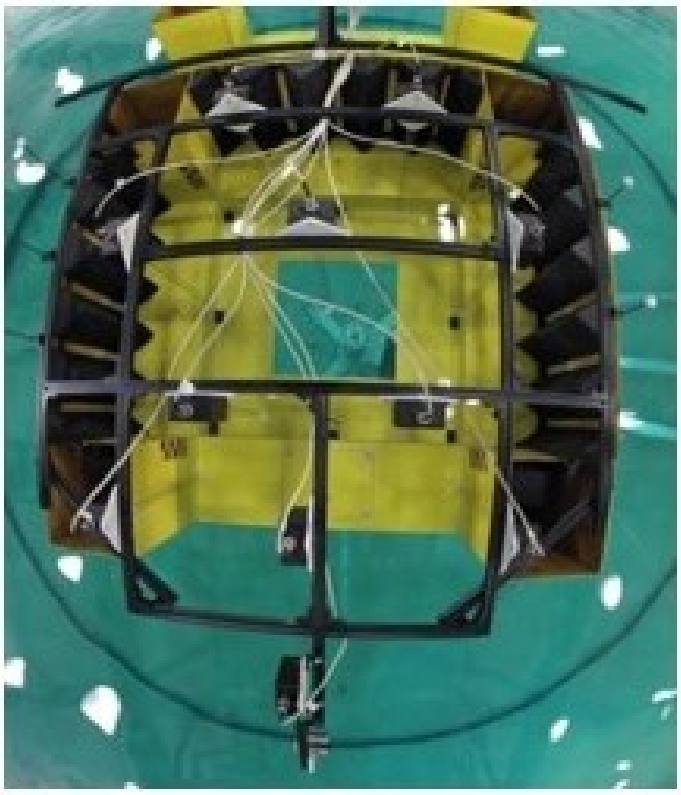

FIGURE 7. Detail concerning the wave probes in the dock.

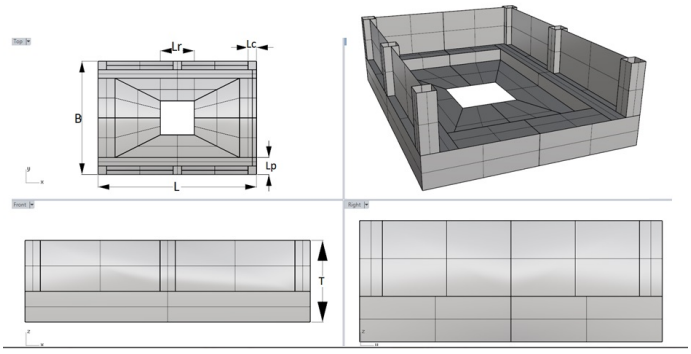

FIGURE 8. 3D mesh for the numerical model.

predictions. The results concerning the relative free-surface elevation can be seen from Fig. 16 to Fig. 20 and the graphs position represents the geometric arrangement of the wave-probes inside the dock in order to simplify the comprehension.

The comparison of the most efficient devices can be verified in Fig.21 and Fig.22 for both 0 and 180^o heading. It should be noticed, mainly for probes 7 and 9 that ES device has a higher attenuation for low period waves. This fact is due to wave scatter, therefore it should be expected less influence of viscous effects and better similarity to full-scale results, which is a good fact since the extrapolation process would be very difficult. This even more evident for 0^o heading.

CONCLUSIONS

It can be verified a good agreement between numerical predictions and experimental results for both wave elevation and body motions, which can be verified from Fig. 9 to Fig. 14 and the relative free-surface elevation from Fig. 15 to Fig. 20.

The semi-submersible has small heave motions for wave periods up of 10 seconds and the absorber devices changed the motions appreciably, changing the wave elevating pattern inside the dock, since body motion also radiate waves inside the dock.

The full side plates configuration (PL) revealled a reduction over 70% in wave internal elevation comparing both 180 to 0 degrees.

The spreaders configuration (ES) showed promising results, providing lower amplitudes compared to the PL configuration for 0 degrees heading for high frequencies, suggesting that there should be an optimum configuration concerning the spreaders arrangements, which will be better investigated by numerical methods, in the next work. It can be also verified that there is two contributions to the internal elevation, the scattered and radiated waves. If the waves are "blocked" by some device, such as the vertical plates, the body motions increase (surge, sway and heave), which produce a high relative elevation due to the hull radiated wave.

ACKNOWLEDGMENT

Thanks to all the TPN staff who assisted in carrying out tests and analyzing the results.

REFERENCES

[1] Oliveira, A. C. d., Vilameá, E. M., Figueiredo, S. R., and Malta, E. B., 2013. "Hydrodynamic moonpool behavior in a monocolumn hub platform with an internal dock". *ASME 2013 32nd International Conference on Ocean, Offshore and Arctic Engineering,* ***Volume 1: Offshore Technology***(2013).

[2] Sheng-Wen Twu, J.-J. D., 1995. "An approach for eliminating re-reflected waves". *Ocean Engineering - OCEAN ENG,* ***22***(5), pp. 421–437.

[3] Twu, S.-W., Liu, C.-C., and Twu, C.-W., 2002. "Wave damping characteristics of vertically stratified porous structures under oblique wave action". *Ocean Engineering,* ***29***(11), Sept., pp. 1295–1311.

[4] Chan, A. T., and Lee, S. W. C., 2001. "Wave characteristics

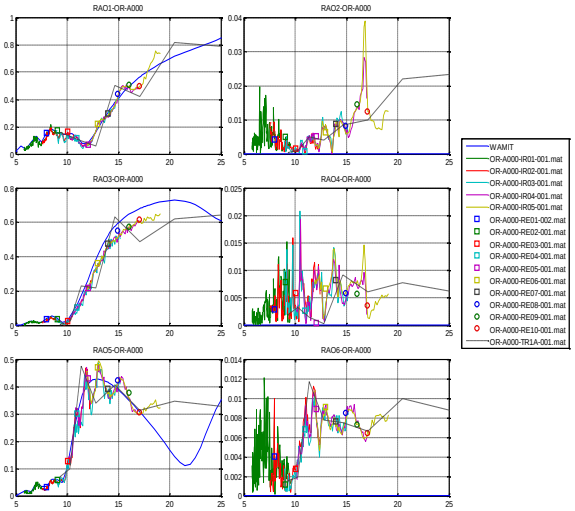

FIGURE 9. RAOs of the floating unit motions at original configuration and wave heading of 0 degrees (waves entering in the dock). X-axis with period in seconds and y-axis RAOs of 1-surge, 2-sway and 3-heave [m/m], 4-roll , 5-pitch and 6-yaw [degrees/m].

past a flexible fishnet". *Ocean Engineering,* ***28***(11), Nov., pp. 1517–1529.

[5] Brossard, J., Jarno-Druaux, A., Marin, F., and Tabet-Aoul, E. H., 2003. "Fixed absorbing semi-immersed breakwater". *Coastal Engineering,* ***49***(12), Aug., pp. 25–41.

[6] Twu, S. W., and Lin, D. T., 1991. "On a highly effective wave absorber". *Coastal Engineering,* ***15***(4), July, pp. 389–405.

[7] Li, Y., Dong, G., Liu, H., and Sun, D., 2003. "The reflection of oblique incident waves by breakwaters with double-layered perforated wall". *Coastal Engineering,* ***50***(12), Nov., pp. 47–60.

[8] Zhu, S., and Chwang, A. T., 2001. "Investigations on the reflection behaviour of a slotted seawall". *Coastal Engineering,* ***43***(2), June, pp. 93–104.

[9] de MELLO, P. C. ; CARNEIRO, M. . T. E. . K. F. . M. R. . A. J. . N. K., 2013. "A control and automation system for wave basins". *Mechatronics (Oxford),* ***23***(12), Nov., pp. 94–107.

[10] WAMIT, Inc. *WAMIT User manual, Version 7.0.* Chestnut Hill, MA. www.wamit.com.

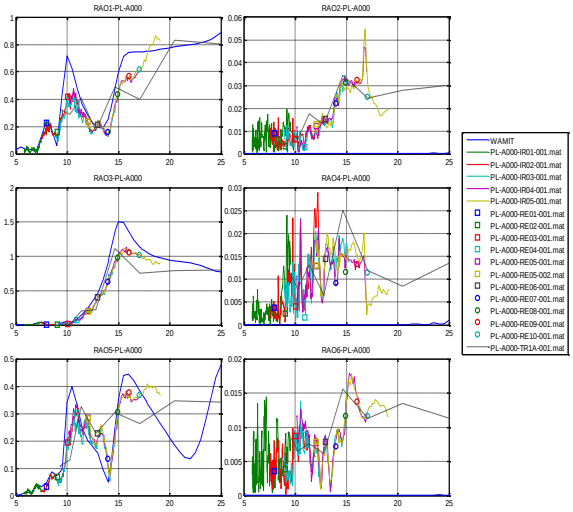

FIGURE 10. RAOs of the floating unit motions with PL configuration and wave heading of 0 degrees (waves entering in the dock). X-axis with period in seconds and y-axis RAOs of 1-surge, 2-sway and 3-heave [m/m], 4-roll, 5-pitch and 6-yaw [degrees/m].

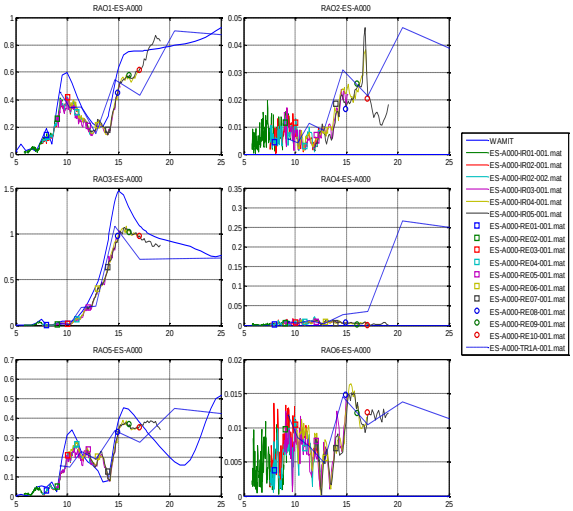

FIGURE 11. RAOs of the floating unit motions with ES configuration and wave heading of 0 degrees (waves entering in the dock). X-axis with period in seconds and y-axis RAOs of 1-surge, 2-sway and 3-heave [m/m], 4-roll, 5-pitch and 6-yaw [degrees/m].

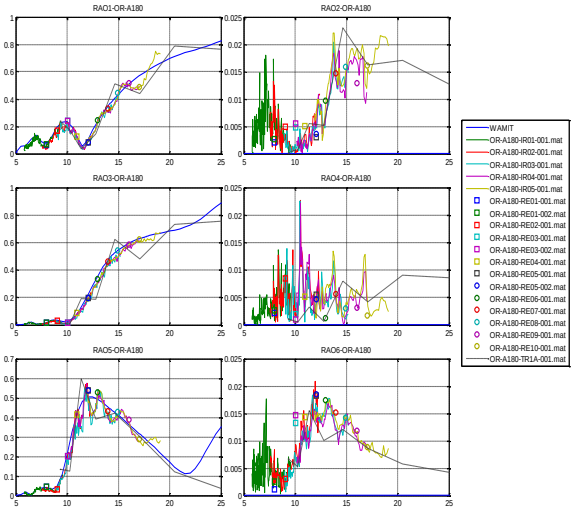

FIGURE 12. RAOs of the floating unit motions at original configuration and wave heading of 180 degrees (dock sheltered). X-axis with period in seconds and y-axis RAOs of 1-surge, 2-sway and 3-heave [m/m], 4-roll, 5-pitch and 6-yaw [degrees/m].

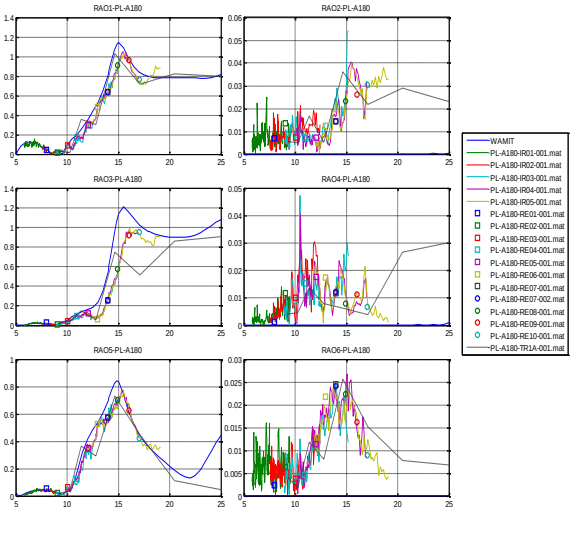

FIGURE 13. RAOs of the floating unit motions at PL configuration and wave heading of 180 degrees (dock sheltered). X-axis with period in seconds and y-axis RAOs of 1-surge, 2-sway and 3-heave [m/m], 4-roll, 5-pitch and 6-yaw [degrees/m].

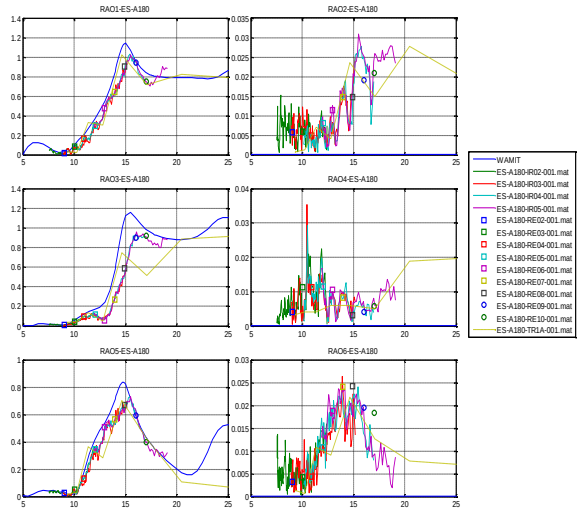

FIGURE 14. RAOs of the floating unit motions at ES configuration and wave heading of 180 degrees (dock sheltered). X-axis with period in seconds and y-axis RAOs of 1-surge, 2-sway and 3-heave [m/m], 4-roll, 5-pitch and 6-yaw [degrees/m].

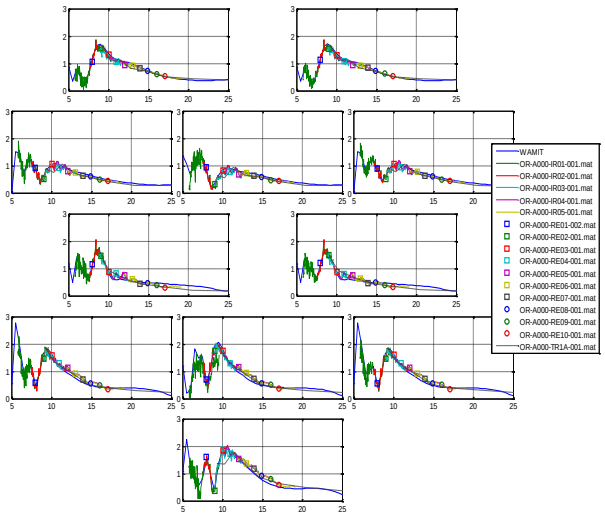

FIGURE 15. RAOs of probes 1-11(arranged as in Fig.6) at original configuration and wave heading of 0 degrees. X-axis with period in seconds and y-axis relative elevation [m/m].

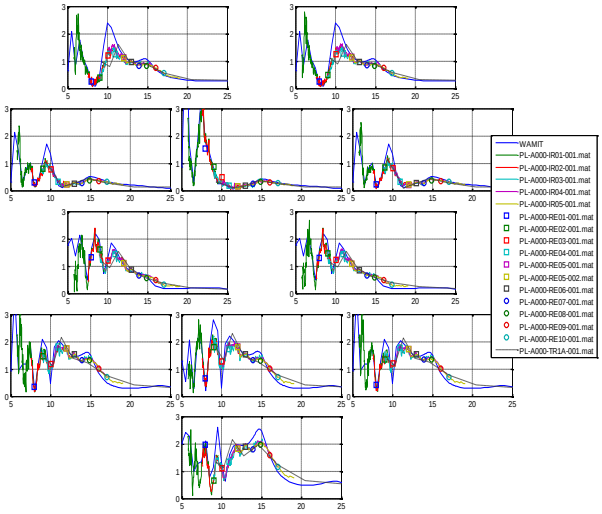

FIGURE 16. RAOs of probes 1-11(arranged as in Fig.6) with PL configuration and wave heading of 0 degrees. X-axis with period in seconds and y-axis relative elevation [m/m].

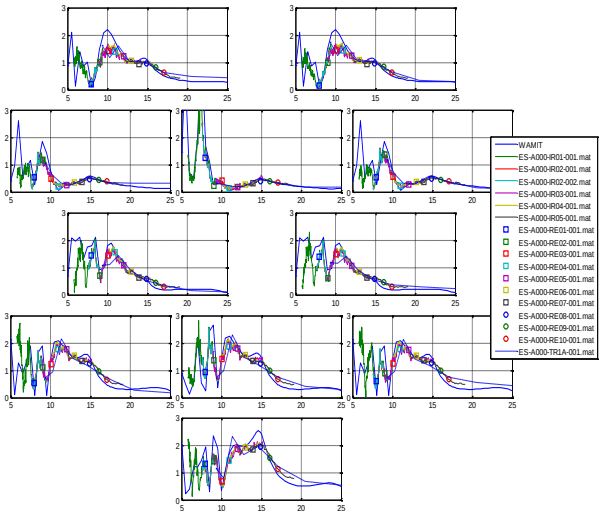

FIGURE 17. RAOs of probes 1-11(arranged as in Fig.6) for RAO-WM-ES-A000 with ES configuration and wave heading of 0 degrees. X-axis with period in seconds and y-axis relative elevation [m/m].

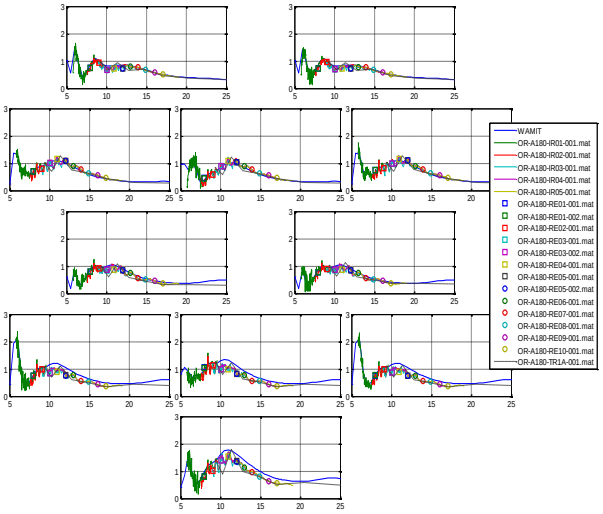

FIGURE 18. RAOs of probes 1-11(arranged as in Fig.6) at original configuration and wave heading of 180 degrees. X-axis with period in seconds and y-axis relative elevation [m/m].

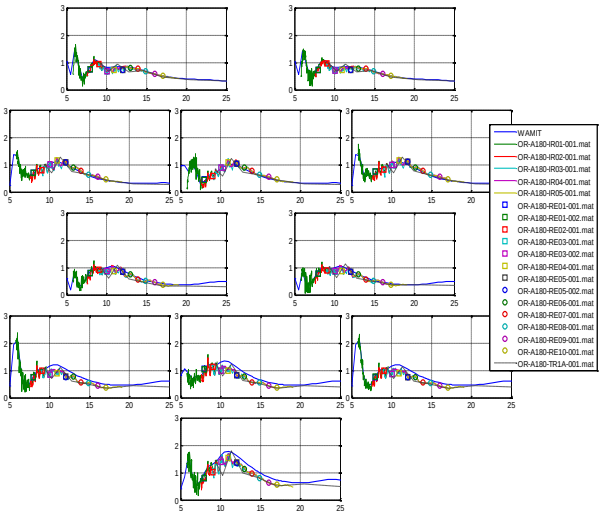

FIGURE 19. RAOs of probes 1-11(arranged as in Fig.6) at original configuration and wave heading of 180 degrees. X-axis with period in seconds and y-axis relative elevation [m/m].

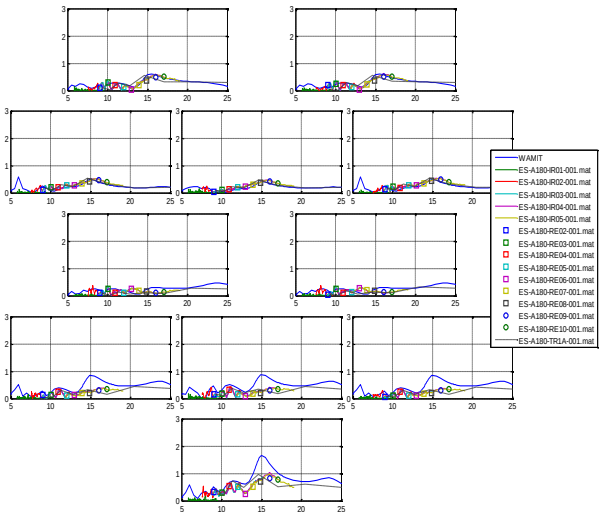

FIGURE 20. RAOs of probes 1-11(arranged as in Fig.6) at ES configuration and wave heading of 180 degrees. X-axis with period in seconds and y-axis relative elevation [m/m].

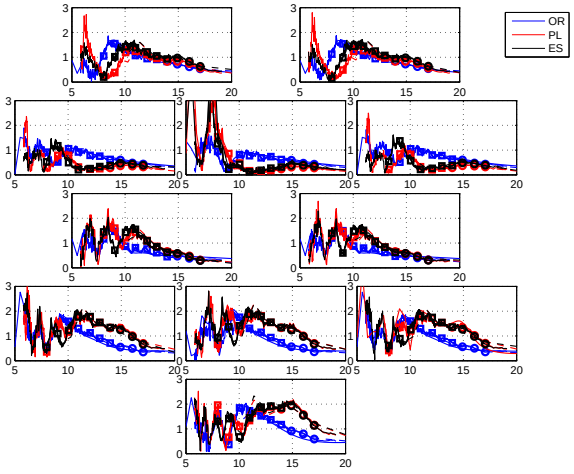

FIGURE 21. RAOs of probes 1-11 (arranged as in Fig.6) at OR,PL and ES configuration for wave heading of 0 degrees. X-axis with period in seconds and y-axis relative elevation [m/m].

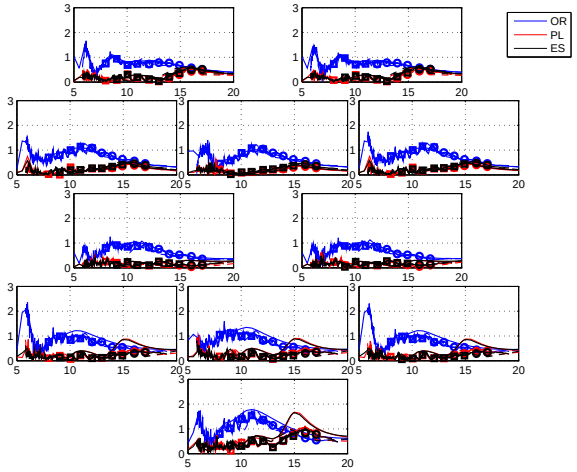

FIGURE 22. RAOs of probes 1-11 (arranged as in Fig.6) at OR,PL and ES configuration for wave heading of 180 degrees. X-axis with period in seconds and y-axis relative elevation [m/m].